On-line determination of Förster resonance energy transfer efficiency in drying latex films: Correlation of interdiffusion and particle deformation

K. Pohl, B. Kussmaul, J. Adams, and D. Johannsmann

Citation: Review of Scientific Instruments **83**, 063103 (2012); doi: 10.1063/1.4726025
View online: http://dx.doi.org/10.1063/1.4726025
View Table of Contents: http://scitation.aip.org/content/aip/journal/rsi/83/6?ver=pdfcov
Published by the AIP Publishing

On-line determination of Förster resonance energy transfer efficiency in drying latex films: Correlation of interdiffusion and particle deformation

K. Pohl, B. Kussmaul, J. Adams, and D. Johannsmann[a)]
Institute of Physical Chemistry, Clausthal University of Technology, D-38678 Clausthal-Zellerfeld, Germany

(Received 28 February 2012; accepted 20 May 2012; published online 8 June 2012)

An instrument is described, which measures the efficiency of Förster resonance energy transfer (FRET) in parallel to the sample's turbidity. The instrument was used to study the film formation from polymer latex dispersions. In this context, the FRET efficiency reflects the diffusion of polymer chains across the interparticle boundaries, while the loss of turbidity reflects the progress of particle deformation. Particle deformation causes tensile in-plane stress, while polymer interdiffusion creates cohesion and thereby helps to prevent cracking. The relative timing between the two therefore is of fundamental importance for successful film formation. The on-line determination of FRET efficiency while the film dries is complicated by the fact that the fluorescence lifetime of the donor, τ_D, depends on the water content in the vicinity of the donor. In the established procedure for data analysis, drifts in τ_D induce corresponding artifical drifts in the values of the FRET efficiency. A novel algorithm for the analysis of fluorescence decay profiles is proposed, which makes use of the method of moments. The FRET efficiency is quantified by the upward curvature of the fluorescence decay curve in log-linear display. In the application example, interdiffusion is delayed relative to particle deformation by about 10 min. For successful film formation, this delay should be as small as possible.
 [http://dx.doi.org/10.1063/1.4726025]

I. INTRODUCTION

Förster resonance energy transfer (FRET) is often employed to study interdiffusion in polymers.[1] Typically, the two types of polymers to be studied are labeled with donor and acceptor moieties, respectively. When the two species intermix, the fluorescence decay profile of the donor changes due to energy transfer from the excited donor to acceptor groups located in the vicinity of the donor. The technique has found much use in the study of the film formation from polymer latex dispersions.[2–4] Diffusion of polymer chains across the interparticle boundaries is important in this context because it is a prerequisite for the build-up of mechanical strength.[5–7] The early experiments of this kind were undertaken on films, which had undergone film formation already and were further aged by thermal annealing.[3] The FRET efficiency was determined on quenched samples as a function of annealing time. Doing the experiment in this way, there are no time constraints on the data acquisition process. Also, the amount of water in the vicinity of the donor (which may affect the fluorescence) is not a problem.

Determining the FRET efficiency while the film dries certainly is interesting, but poses severe challenges. First, data acquisition must be faster than the drying process itself. This is possible (albeit with some difficulty) using modern UV LEDs, which have a repetition rate in the MHz range.[8,9] A second problem is the artifacts related to variable water content. Finally, the kinetics of the FRET efficiency can only be interpreted, if it is correlated with other parameters relevant to film formation. Since drying usually proceeds from the edge of the film towards the center, these parameters must be measured at the exact same spot as the FRET efficiency. Otherwise, the relative timing would not be meaningful. A useful parameter of this kind is the whiteness of the film. At the time when the film becomes clear, the contacting particles deform and the interstitial voids disappear. The loss of void volume leads to tensile stress. If the cohesion between particles develops early enough, the film can withstand this tensile stress. Otherwise, it will crack.[10,11] It is therefore desirable to design the material in such a way that interdiffusion sets in immediately after interparticle contact. We show in Sec. III that such a correlation can be established by measuring the scattered light in parallel to the FRET efficiency with a second channel in the detection system.

A severe problem with FRET measurements on drying films is the dependence of the donor lifetime on water content. A drift of donor lifetime, τ_D, causes artifacts in the analysis of the decay curves if these are fitted with the widely used two-state model.[3] We propose a novel formalism to quantify the FRET efficiency based on the method of moments in Sec. IV. This algorithm is robust against drifts in the donor lifetime. We conclude with an application example in Sec. V.

II. SAMPLE PREPARATION

Polymer latexes were prepared by miniemulsion polymerization. The monomers used were methylmethacrylate (MMA, Aldrich, > 99%), butylacrylate (BA, Aldrich, 99%), and acrylic acid (AA, Fluka, 99%). Hexadecane (HD, Aldrich, 99%) was added as the costabilizer and azo-*bis*-isobutyronitrile (AIBN, recrystallized from ethanol)

[a)]Author to whom correspondence should be addressed. Electronic mail: johannsmann@pc.tu-clausthal.de.

TABLE I. Sample properties.

Sample	MMA/BA ratio (wt.%)	T_g (°C)	r_H (nm)	Surfactant	Labeling
A	40:60	− 10	70	Dowfax 2A1, 2 wt.%	Donor
B	50:50	4	53 (D) 54 (A)	SDS, 2 wt.%	Donor and acceptor
C	35:65	− 16	47 (D) 54 (A)	SDS, 2 wt.%	Donor and acceptor

as the initiator for polymerization. As the donor/acceptor pair, we used phenanthrene methylmethacrylate (Phe-MMA, Toronto Research Chemicals) and [1-(4-nitrophenyl)-2-pyrrolidinemethyl]-acrylate (NPP-A, Aldrich, 97%). Both contain polymerizable groups and are incorporated into the polymer chains, thereby ensuring that the labels reflect the movement of the polymer chains. The Förster distance for this pair is 2.47 nm.[12] NPP-A is a non-fluorescent acceptor, which is advantageous because it avoids a possible interference between acceptor fluorescence with the donor fluorescence in the detection process.

Preparation parameters for the three different samples are provided in Table I. The MMA/BA ratio determines the softness of the polymer. The glass temperatures given in Table I were calculated from the T_g's of the pure components (105 and −54 °C for PMMA and PBA, respectively[13]) with the Fox equation.[14] AA, HD, and AIBN were always added in amounts of 1.5, 4, and 1.5 wt.% (based on monomer), respectively. We always prepared two batches containing either the donor, Phe-MMA, 1.7 wt.% or the acceptor, NPP-A, 1 wt.%. A lower acceptor concentration was chosen for reasons of cost. In case of sample A, only the batch containing the donor was used in experiment in order to determine the donor lifetime in the absence of the acceptor. For samples B and C, donor-labeled and acceptor-labeled batches were mixed in a volume ratio of 1:1. The surfactants employed were Dowfax 2A1 (Dow) for sample A and sodiumdodecylsulfate (SDS, Sigma Aldrich, 99%) for samples B and C. Organic phase and aqueous phase were mixed with a magnetic stirrer and sonicated (Branson Sonifier 450, output 70%) for 2 min. The resulting miniemulsions were polymerized for 20 h at 70 °C. The final solids content was 20 wt.%. Particle radii for donor and acceptor labeled latexes as determined with dynamic light scattering were the same within ±10 nm (see Table I).

Films were formed by manually spreading the latex dispersion onto a glass slide. The wet thickness was 180 μm. Drying occurred at room temperature (22−24 °C) and under controlled humidity, where the humidity was adjusted to 70% rH by mixing a dry and a vapor saturated air stream.

For data analysis with the two state model (see Sec. IV), one needs to know the donor lifetime and the acceptor concentration. The latter is contained in the parameter γ in (1) and (2). The donor lifetime, τ_D, was determined in a reference experiment on a sample, which only contained donors. The decay curves were fitted with single exponentials. Interestingly, the donor lifetime changed during drying. We come back to this problem in Sec. IV. For the determination of the parameter γ, a film was prepared from a mixture of donor-labeled and acceptor-labeled polymers, which had been dissolved in tetrahydrofurane (THF, Riedel-de Häen). This condition provides for maximum intermixing. γ was determined by fitting the decay curves with the Förster law:

$$\frac{I_D(t)}{I_{D0}} = \exp\left(-\frac{t}{\tau_D} - 2\gamma\sqrt{\frac{t}{\tau_D}}\right). \quad (1)$$

$I_D(t)$ is the fluorescence intensity versus time ("decay profile"), I_{D0} is the peak of the decay profile, and $\gamma = 4\pi^{3/2}/6\, R_F{}^3\, C_A$ (R_F the Förster radius) and quantifies the acceptor concentration, C_A, next to a donor.

III. SIMULTANEOUS DETECTION OF SCATTERED LIGHT AND FRET EFFICIENCY

Any physical interpretation of the kinetics of FRET efficiency must in one way or another correlate the FRET efficiency to other drying parameters. Most important among the other parameters are stress and particle deformation. We focus on particle deformation here. There is an easily accessible parameter reflecting particle deformation, which is the turbidity of the film. When the spheres deform into polyhedra, the interstitial voids disappear and the amount of light scattered from the sample decreases. Clearly, there is no simple quantitative relation linking the amount of scattered light to the degree of particle deformation. Scattered light here only serves as an indicator for the kinetics of deformation, which is to be compared to the kinetics of FRET efficiency.

Monitoring the intensity of scattered light in parallel to the FRET efficiency amounts to a simple modification of the setup. We implemented a second detection channel and equipped the two channels with color filters such that the first channel mainly detects fluorescence, while the second only detects scattered light. In principle, the second channel provides the pulse shape of the LED as well, but the only parameter used for further analysis here is the integral number of photons in this channel. Note that this measurement occurs at the exact same spot as the measurement of the FRET efficiency, which is essential because there is a moving drying front.

Figure 1 shows a diagram. The light passing through the light guide is split into two beams. Color filters are employed, selecting fluorescent light on channel 1 and scattered light on channel 2. Excitation occurred with a pulsed UV LED (PicoQuant GmbH, $\lambda = 283$ nm, repetition rate 2 MHz). The irradiated spot has a diameter of 1 mm. Fluorescence decay profiles were acquired by means of time correlated single photon counting (TCSPC, EG&G ORTEC). The instrument produces

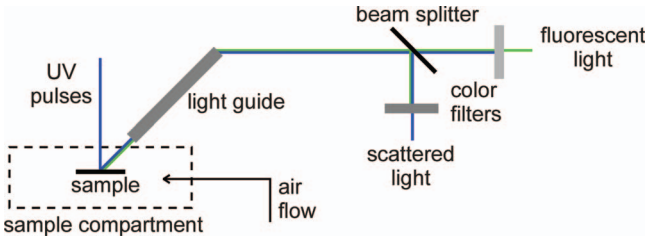

FIG. 1. Experimental setup. Fluorescent and scattered light are simultaneously detected from the same spot on the film.

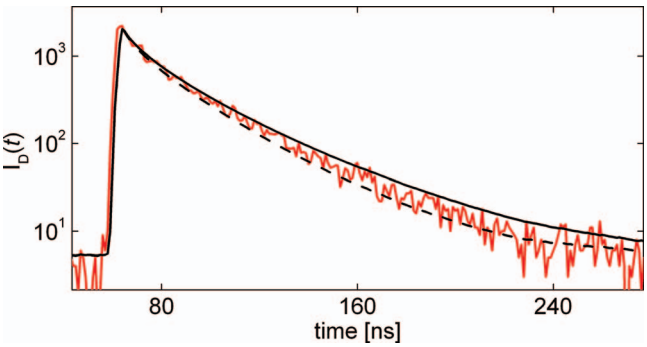

FIG. 2. Typical fluorescence decay curve. The lines are predictions from the two state model. The parameters are $\tau_D = 43$ ns, $A_2 = 0.9$, $\gamma = 0.7$, $\chi^2 = 8.1$ for the full line and $\tau_D = 45$ ns, $A_2 = 1$, $\gamma = 0.7$, $\chi^2 = 7.1$ for the dashed line. These sets of parameters fit the data about equally well and the errors in A_2 and τ_D in consequence are correlated.

a histogram of the number of photons versus arrival time. The accumulation time was 30 s, which implies a time resolution of 2 data points/min. The drying time was around 2 h (cf. Figs. 4 and 5).

IV. DETERMINATION OF FRET EFFICIENCY BY THE METHOD OF MOMENTS

Before describing the proposed novel method for analysis, we briefly elaborate on the procedure widely used at present and on why this procedure poses problems if the water content varies. Usually, one fits the fluorescence decay curve with a suitable fit function. However, the underlying physics is so complicated that a realistic fit function would have to contain many free parameters.[15] Since such a large parameter space is impractical, a simple two-state model is often employed.[3] Within this model, a fraction A_2 of donor molecules exhibits FRET, while a second fraction $(1-A_2)$ does not. "Exhibits FRET" here implies a single, fixed acceptor concentration in the vicinity of the respective donor molecule (a single, fixed parameter γ in (2)). The two-state model is unrealistic because the acceptor concentration around any given donor gradually increases as interdiffusion progresses. Nevertheless, the two-state model may serve as a heuristic fit function. Of course, A_2, as derived from fitting with this model, should not be quantitatively interpreted as the fraction of labels having crossed the boundaries. A_2 is an indicator of interdiffusion.

Following the two-state model, the decay profile amounts to a superposition of two terms, which are a single exponential and a term of the Förster form:

$$\frac{I_D(t)}{I_{D0}} = (1-A_2)\exp\left(-\frac{t}{\tau_D}\right) + A_2\exp\left(-\frac{t}{\tau_D} - 2\gamma\sqrt{\frac{\mathrm{t}}{\tau_D}}\right). \tag{2}$$

In principle, there are four free parameters (I_{D0}, A_2, γ, τ_D), but one usually keeps γ fixed.

There is a drawback to (2), which is unrelated to molecular interpretation. When fitting experimental decay curves with (2), one finds that the errors in A_2 and τ_D are correlated. Figure 2 shows an example. The fluorescence decay curve shows an upward curvature in log-linear display, which is the characteristic signature of energy transfer. However, fitting these data with (2) does not yield a unique result. The underlying problem is that the data systematically differ from (2). The χ^2-landscape under such conditions usually consists of an elongated ellipse in the τ_D-A_2-plane. Fixing either A_2 or τ_D, one can determine the other parameter with good precision (better than 10%). However, if A_2 and τ_D are both free, there is a large uncertainty on the derived values. The problem is not of much concern as long as the donor lifetime stays constant during drying. One may then maintain τ_D fixed in the fit. Even if the value of τ_D is subject to debate, *changes* in the derived values for A_2 can then be safely attributed to interdiffusion. However, τ_D is not constant during drying (Fig. 4). A dependence of τ_D on water content can come about by different mechanisms, mostly related to the local polarity and the local refractive index. The fact that τ_D drifts necessitates a formalism for data analysis, which is robust against variable τ_D.

On a qualitative level, the signature of energy transfer is the upward curvature of the decay curve in log-linear display (cf. Fig. 2). In the absense of energy transfer, the fluorescence decay in log-linear display is a straight line. Energy transfer makes the decay function non-exponential. In the following, we propose the use of a "non-exponentiality parameter," P_{NE}, to quantify this upward curvature. P_{NE} is defined using the method of moments,[16,17] and its calculation therefore is model-free. The moments of the fluorescence decay curve, $I_D(t)$, are defined as

$$a_0 = \int_{t_{\min}}^{t_{\max}} I_D(t)\,\mathrm{d}t, \quad a_1 = \int_{t_{\min}}^{t_{\max}} t\, I_D(t)\,\mathrm{d}t,$$
$$a_2 = \int_{t_{\min}}^{t_{\max}} t^2\, I_D(t)\,\mathrm{d}t. \tag{3}$$

P_{NE} is defined as

$$P_{NE} = \frac{a_2/a_0}{(a_1/a_0)^2}. \tag{4}$$

Calling t the decay time of a single fluorophore, the numerator is equal to $\langle t^2\rangle$ and the denominator is $\langle t\rangle^2$. (Angular brackets denote averaging.) P_{NE} is equal to $\langle t^2\rangle/\langle t\rangle^2$. Ideally, the integration in (3) would start at $t_{min} = 0$ and run to $t_{max} = \infty$. In practice, it must start at some finite time $t_{min} > 0$ in order to avoid a non-exponentiality originating from the folding of the decay curve with the excitation pulse. The upper limit t_{max} is chosen such that the noise in $I_D(t)$ at large times is limited in its influence on P_{NE}. For an exponential decay of the form $\exp(-t/\tau_D)$ and integration from zero to

infinitiy, one has $P_{NE} = 2$. If $I_D(t)$ has an upward curvature in log-linear display, P_{NE} becomes larger than 2. However, P_{NE} may also be less than 2 for non-ideal integration limits t_{min} and t_{max}. If the decay function follows the two-state model (2), the integrations in (3) can still be done analytically. The result is

$$P_{NE} = \frac{(1 + A_2\alpha\gamma)(8 + A_2\gamma(18\gamma + 4\gamma^3 + \alpha(15 + 20\gamma^2 + 4\gamma^4)))}{(2 + A_2\gamma(2\gamma + \alpha(3 + 2\gamma^2)))^2}$$
$$\alpha = \sqrt{\pi}\exp(\gamma^2)(\mathrm{erf}(\gamma^2) - 1). \quad (5)$$

Clearly, P_{NE} is independent of the donor lifetime, τ_D.

In principle, the non-exponentiality parameter picks up all deviations from Eq. (1). However, P_{NE} is most useful, when there is an upward curvature in the decay plots. P_{NE} was defined such that it quantifies this curvature. An upward curvature is an indicator of energy transfer and P_{NE} is a good measure of the amount of energy transfer. Should the curvature be negative (which is not expected, but of course possible, in principle), one would have to step back and discuss the underlying physical reason. P_{NE} will also capture negative curvature (the values will decrease) but discussing P_{NE} for such situations will not give a physical insight.

As a side remark, we comment on the influence of a non-zero background. No background was subtracted from the data shown in Fig. 2. A non-zero background of course also produces an upward-curvature. However, this upward curvature occurs at low count rates (late times). It is not indicative of energy transfer. The relevant section of the plot is the time shortly after the excitation pulse. When manually inspecting data, distinction between decays with and without energy transfer occurs based on the early portion of the curve. When calculating P_{NE}, the integration range is chosen such that the background has little influence on the derived P_{NE}. The lower integration boundary, t_{min}, was chosen as 79 ns. The upper integration boundary, t_{max}, was chosen at a time before the signal converges to the background (260 ns).

In a first step of validation, the method of moments was tested on simulated decay curves. We started from decays as given in (2) with $\gamma = 0.7$, $A_2 = 0.2$, and varied τ_D between 43 and 45 ns. These decays were folded with the excitation pulse, where the latter had a half-width of 1 ns. A background of 0.04% relative to the peak intensity and Gaussian noise with a standard deviation of 0.012% of the peak intensity were superimposed onto this curve. We then fitted the two-state model to this set of simulated data. In these fits, A_2 was the free parameter, while τ_D was fixed at 44 ns. Since this latter value is different from the values used in the simulation, there are systematic errors. The fit routine compensates for the mismatch in the lifetimes by adjusting A_2. The results are shown as open squares in Fig. 3. A variability of τ_D in the simulated data does affect the derived values of A_2. This problem is avoided with the method of moments (open circles in

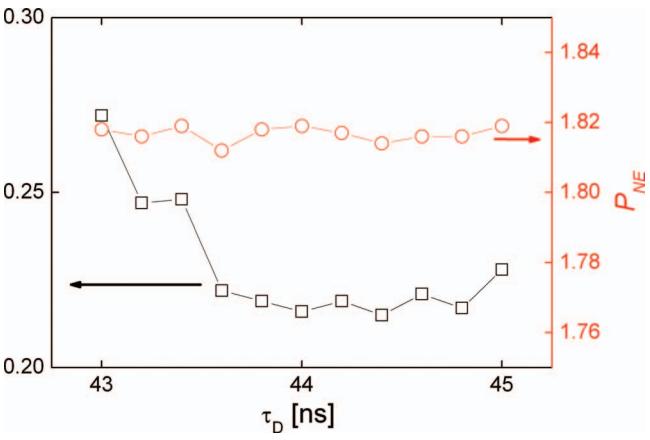

FIG. 3. Results from a simulation, where synthetic data were produced with $I_D(t)$ following the two-state model. For the simulated data, γ and A_2 were maintained fixed at values of 0.7 and 0.2. τ_D was varied between 43 and 45 ns. In the fit procedure, τ_D was maintained fixed at 44 ns and A_2 was allowed to vary in order to minimize χ^2. Clearly, if the true lifetime is shorter than the value assumed in the fit, the fit compensates for this mismatch by increasing A_2. This problem does not occur with the method of moments. The non-exponentiality parameter shows no systematic dependece on τ_D.

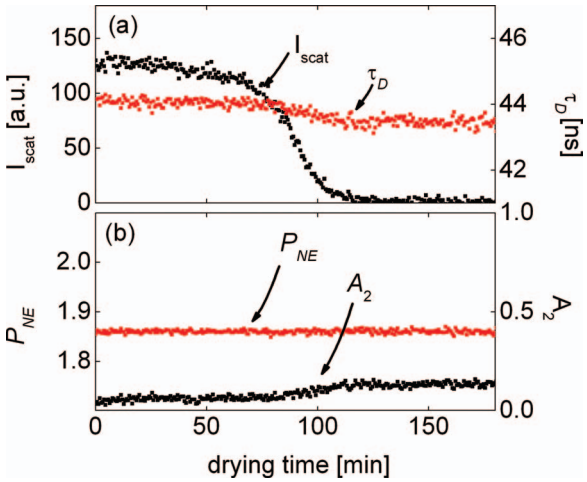

FIG. 4. Data acquired from a film drying experiment with a latex containing only donor molecules. (a) Scattering intensity and donor lifetime as derived by fitting the decay curves with single exponentials. (b) FRET efficiencies as determined from the two-state model (A_2) and by the method of moments (P_{NE}). While the parameter A_2 displays a step at the time where the donor lifetime decreases, no corresponding step is seen in P_{NE}. P_{NE} is the more robust parameter.

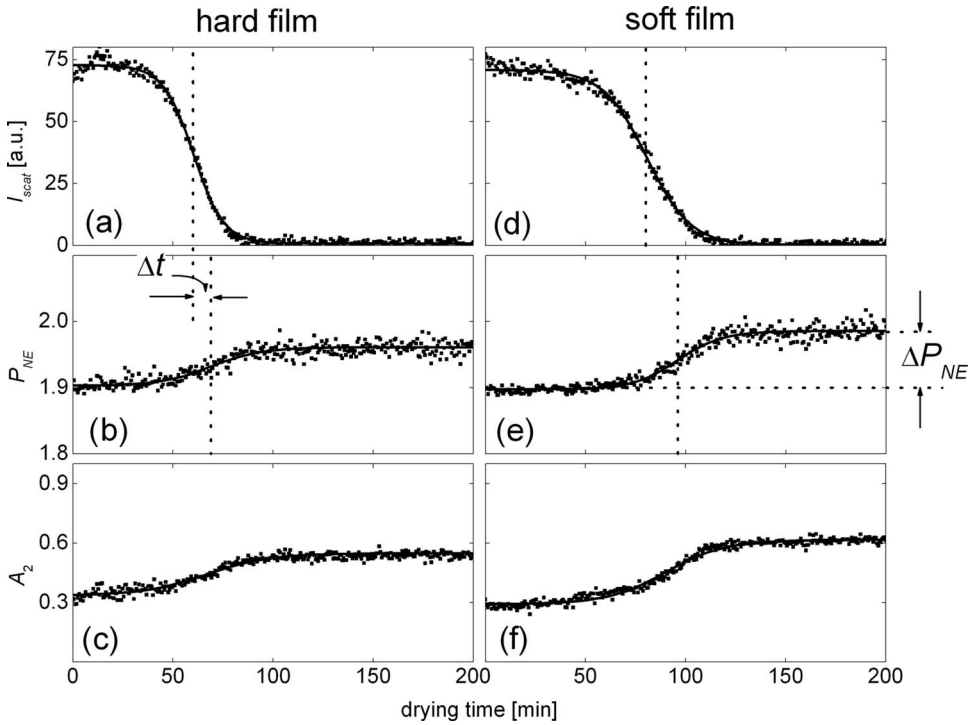

FIG. 5. Scattering efficiency (a, d), FRET efficiency P_{NE} (b, e) and A_2 (c, f) as a function of the drying time for a hard film (50 wt.% MMA, (a–c)) and a soft film (35 wt.% MMA, (d–f)). The lines are fits with Eq. (6). Δt is the time difference between the inflection points found for scattering and interdiffusion. Δt should be as small as possible in order to achieve internal cohesion in the film at the time when the stress is at its maximum. The second parameter to be optimized is the jump in the non-exponentiality parameter. ΔP_{NE} should be as high as possible. Panels c and f are similar to panels b and e. The fluctuations in A_2 actually are smaller than the fluctuation in P_{NE}. Still, the parameter P_{NE} is not affected by drifts of the donor lifetime and therefore is considered to be the more reliable indicator for FRET efficiency.

Fig. 3). The non-exponentiality parameter is constant within the noise.

A second step of validation was undertaken with experimental data, where the latex only contained donor groups (Fig. 4). Fitting all decay curves with simple exponentials, we find that the donor lifetime slightly decreases during drying. If one ignores this variability of τ_D and fits the data with (2) and fixed τ_D, one finds an increase of A_2 with drying time. This is an artifact. Again, the problem is solved by use of the method of moments. Clearly, P_{NE} is not affected by the changes in τ_D.

V. APPLICATION EXAMPLE

We conclude with two examples demonstrating the benefits of the proposed methods. Figure 5 shows the scattering intensity (a and d) and the non-exponentiality parameter (b and e) for samples B and C from Table I. The dependence of A_2 on drying time is shown for comparison in panels c and f. Both materials are stabilized with 2 wt.% SDS. They differ in the softness of the polymer.

The time evolution of scattering intensity, I_{Scat}, and FRET efficiency, P_{NE}, is sigmoidal. The data were fitted with the functions

$$I(t) = I_{ini} - \Delta I \frac{1}{2}\left(\tanh\left(\frac{t - t_{cen,I}}{w_I}\right) + 1\right)$$

$$P_{NE}(t) = P_{NE,ini} + \Delta P_{NE} \frac{1}{2}\left(\tanh\left(\frac{t - t_{cen,P}}{w_P}\right) + 1\right). \quad (6)$$

The index *ini* denotes the initial state. Δ denotes the amplitude of the step. t_{cen} is the time of the inflection point and w is the width of the step. Central to physical interpretation are the differences between the inflection points, $\Delta t = t_{cen,P} - t_{cen,I}$, and the step height of the FRET efficiency, ΔP_{NE}. Δt should be small, that is, interdiffusion should set in immediately after the first interparticle contact. ΔP_{NE} should be as large as possible. Of course, a large amplitude, ΔP_{NE}, can always be achieved with soft polymers (such as sample C), but this comes at the expense of a correspondingly soft film. The values obtained from fitting (6) to the data shown in Fig. 5 are $\Delta t = 9$ and 16 min and $\Delta P_{NE} = 0.058$ and 0.088 for the hard and the soft sample (B and C in Table I), respectively. Further results covering a wider set of preparation conditions will be provided in a separate communication.

VI. CONCLUSIONS

Using a second detection channel in a standard TCSPC equipment, we have determined the turbidity of a drying latex film in parallel to its FRET efficiency. These two parameters reflect particle deformation and interdiffusion, respectively. In order to circumvent artifacts in the analysis of the fluorescence decays originating from variable donor lifetime, we have quantified the FRET efficiency by a non-exponentiality parameter. The central parameters for physical interpretation are, first, the delay between the steps in scattering efficiency and FRET efficiency and, second, the amplitude of the step in

FRET efficiency. This instrument allows to correlate particle deformation and interdiffusion on drying latex films.

ACKNOWLEDGMENTS

We acknowledge technical help by Maria Sonnenberg and Lisa Sarah Müller as well as financial support by the DFG (Contract No. DFG Jo278/18-1).

[1]C. L. Zhao, Y. C. Wang, Z. Hruska, and M. A. Winnik, Macromolecules **23**, 4082 (1990).
[2]O. Pekcan, M. A. Winnik, and M. D. Croucher, Macromolecules **23**, 2673 (1990).
[3]Y. C. Wang, C. L. Zhao, and M. A. Winnik, J. Chem. Phys. **95**, 2143 (1991).
[4]Y. C. Wang and M. A. Winnik, J. Phys. Chem. **97**, 2507 (1993).
[5]J. Keddie and A. F. Routh, *Fundamentals of Latex Film Formation: Processes and Properties* (Springer, 2010).
[6]S. S. Voyutskii, J. Polym. Sci. **32**, 528 (1958).
[7]A. Zosel and G. Ley, Macromolecules **26**, 2222 (1993).
[8]A. Turshatov, J. Adams, and D. Johannsmann, Macromolecules **41**, 5365 (2008).
[9]W. F. Schroeder, Y. Q. Liu, J. P. Tomba, M. Soleimani, W. Lau, and M. A. Winnik, Polymer **52**, 3984 (2011).
[10]M. S. Tirumkudulu and W. B. Russel, Langmuir **21**, 4938 (2005).
[11]W. P. Lee and A. F. Routh, Langmuir **20**, 9885 (2004).
[12]A. Turshatov and J. Adams, Polymer **48**, 7444 (2007).
[13]J. Brandrup, E. H. Immergut, and E. A. Grulke, *Polymer Handbook*, 4th ed. (Wiley, 1999), pp. V/88–VI/199.
[14]P. Mischke, *Filmbildung* (Vincentz Network, Hannover, 2007).
[15]A. Dhinojwala and J. M. Torkelson, Macromolecules **27**, 4817 (1994).
[16]A. A. Istratov and O. F. Vyvenko, Rev. Sci. Instrum. **70**, 1233 (1999).
[17]I. Isenberg and R. D. Dyson, Biophys. J. **9**, 1337 (1969).